

## Random telegraph signals from liquid helium to room temperature

D. H. Cobden<sup>a</sup> and M. J. Uren<sup>b</sup>

<sup>a</sup>Cavendish Laboratory, Madingley Road, Cambridge CB3 0HE, UK

<sup>b</sup>Defence Research Agency, Great Malvern, Worcestershire WR14 3PS, UK

The noise in unstressed MOSFETs at temperatures as low as 1.2 K is produced mainly by electron-trapping defects, as it is at room temperature. However, the defects active at low temperatures lie closer to the Si/SiO<sub>2</sub> interface, showing a preference for particular effective depths (2.2 and 5.5 Å) into the oxide, and they influence the conductance mainly by scattering rather than number density modulation. After electrical stress many more defects are active, and their interaction with the conduction electrons is very complex. A new type of defect is detected amongst them which acts not as an electron trap but as a two-state system, producing random telegraph signals whose time constants show dramatic resonances as a function of gate voltage.

### 1. INTRODUCTION

The flicker noise in MOSFETs at room temperature is caused mainly by random changes in charge state of defects near the Si/SiO<sub>2</sub> interface. In submicron devices the noise often takes the form of switching between only two discrete constant resistance levels, each corresponding to a different charge state of a single defect. The time constants of such a random telegraph signal (RTS) are the reciprocals of the quantum transition rates for electron capture and emission, while the RTS amplitude depends on the interaction between the defect and the inversion layer carriers.

Although RTSs in MOSFETs were first studied at liquid helium temperatures [1], almost all subsequent work has been in the temperature range above 77 K. However, the different conditions at liquid helium temperatures can provide very useful complementary information. The defects visible at room temperature show activated behaviour, so at 4.2 K they are frozen out. The RTSs visible then are related to defects whose transition rates would be very fast at room temperature. The low thermal energy and the consequent degeneracy of the inversion layer simplify the treatment of defect energy levels, and allow greatly improved resolution in energy. The conduction processes are also modified, as phonon scattering is frozen out, electron-electron scattering is reduced and the transport becomes two-dimensional, so the way in which the defects influence the resistance is also different at low temperatures.

### 2. DEVICES AND MEASUREMENTS

The devices used were conventional 1.5 μm-process n-channel MOSFETs, without low-doped drains, having electrically active areas of about 1 μm<sup>2</sup>, oxide thickness  $d_{ox}=320$  Å and initial threshold gate voltage 0.7 V. Much lower signal levels must be used than at room temperature to eliminate electron heating effects – the source-drain voltage should be not larger than  $k_B T/e$ , where  $T$  is the temperature, ie, a few hundred μV. The resistance was measured with a maximum time resolution of about 200 μs on a carefully screened pumped-helium

cryostat down to 1.2 K using an ac constant-current technique. When measured separately, the time constants  $\tau_1$  and  $\tau_2$  for respectively the higher and lower resistance levels of an RTS were obtained by averaging over at least 500 transitions, giving a standard error of less than 5%.

A variety of electrical stressing techniques were investigated. Most effective for producing RTSs was the application of a large positive drain bias, either at room temperature or at 4.2 K. As the degree of stress was increased, the threshold voltage became more and more positive and the reproducible random structure in the characteristics became larger. This was due to injection of electrons into the oxide near the drain, so that the conductance was dominated more and more by a very small region with large potential fluctuations adjacent to the drain [2].

### 3. ELECTRON TRAPS

Fig. 1 shows the quantity  $\tau_1/\tau_2$  plotted against  $V_g$  for four different two-level RTSs in unstressed devices at 4.2 K. In agreement with previous work [1,3] we find that at low temperatures  $\tau_1/\tau_2$  is always exponential in  $V_g$ , that is,

$$\tau_1/\tau_2 = \exp[es\eta(V_g - V_{g0})/k_B T] = \exp(-\Delta E/k_B T), \quad (1)$$

where  $e$  is the electronic charge,  $s = \pm 1$  is the "polarity" [1],  $\eta$  is a positive constant, and  $V_{g0}$  is the gate voltage at which  $\tau_1 = \tau_2$ . The equality  $\tau_1/\tau_2 = \exp(-\Delta E/k_B T)$  is the usual statement of detailed balance, and hence the energy parameter  $\Delta E = -es\eta(V_g - V_{g0})$  is linear in  $V_g$ . For such RTSs,  $\tau_1$  and  $\tau_2$  individually always vary monotonically with  $V_g$ . These facts agree with the simple model depicted in Fig. 2, where electrons tunnel backwards and forwards from near the Fermi energy  $E_F$  in the inversion layer to a near-interface oxide defect with energy  $E_t$  lying above the bottom of the silicon conduction band. In this model the change in resistance on electron capture is  $s\Delta R$ , where  $\Delta R$  is the amplitude of the RTS, and  $\Delta E = E_t - E_F$ . As the inversion layer contains a degenerate Fermi distribution  $f(E)$ ,  $E_F$  is practically constant in strong inversion, and also the typical range of  $V_g$  over which an RTS is visible is only about 200 mV. Therefore  $\eta$  can be related directly to an effective depth  $d_t = |dE_t/d(eV_g)| = \eta d_{ox}$  of the defect into the oxide, although this is not the true distance from the interface as the surface potential must also change to some extent with  $V_g$ .

At room temperature all RTSs are of positive polarity, ie  $s = +1$ , as expected if the interaction of the defect with the electrons is dominated by number-density modulation. As  $V_g$  increases,  $E_t$  moves down past  $E_F$  and the trap fills up, so the number of

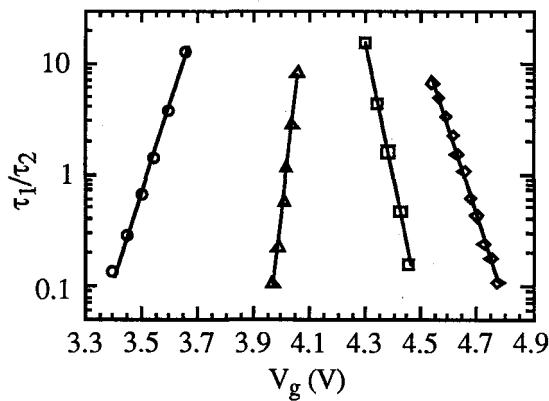


Figure 1. Gate-voltage dependence of the up-down ratio of four RTSs in unstressed devices:  $\circ$  A20N18b,  $\Delta$  B4N21a,  $\square$  A20N18a, and  $\diamond$  A15N17. Solid lines are best fits to Eqn. (1).

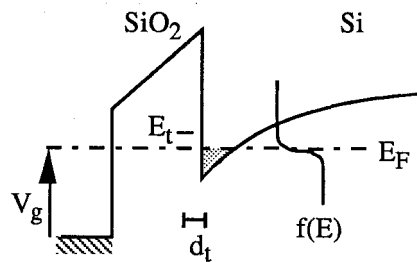


Figure 2. Schematic band diagram of an n-channel MOSFET at low temperature, showing a single electron trap in the oxide.

electrons in the inversion layer decreases to balance the trapped charge and the resistance goes from the low ( $\tau_2$ ) to the high ( $\tau_1$ ) state. Fig. 3 displays values of  $d_t$  and  $s\Delta R$  for fifteen randomly chosen RTSs in strong inversion in unstressed devices at 4.2 K, sorted in order of  $d_t$ .  $\Delta R$  is typically of the order of  $0.5 \Omega$ , corresponding to  $\Delta R/R$  of order  $5 \times 10^{-4}$ , which is an order of magnitude larger than expected from number density modulation [3]. Also, a third of these RTSs have negative polarity, ie  $s=-1$ , which is completely inconsistent with a number density effect. The value of  $s\Delta R$  must therefore be attributed mainly to a change in scattering cross-section, which may either increase or decrease on electron capture. In these devices, quantum interference effects [4] are small above 1.2 K, as evinced by the low sensitivity of  $R$  and  $\Delta R$  to magnetic field ( $<1\%$  change up to 4 T). The change in scattering amplitude from an electron trap should therefore be considered as a local interference effect [5], which is consistent with  $s\Delta R$  being randomly distributed over a certain range, as in Fig. 3 (a), as a result of the accidental positioning of other scatterers in the device relative to the trap.

It is apparent from Fig. 3 (b) that the transfer distance  $d_t = \eta d_{ox}$  is usually smaller than the minimum of about  $10 \text{ \AA}$  found at room temperature. The total transition rate depends on the tunnelling probability for the electron into the defect and on the probability for any accompanying lattice reconfiguration. Because the latter is normally assisted by phonons at higher  $T$ , we might expect its probability to be smaller on average at low  $T$ , where the lattice can only reconfigure by tunnelling. If this is the case then only defects lying closer to the interface, with a higher electron tunnelling probability, can have sufficiently high transition rates to produce RTSs. More surprisingly perhaps, there is a distinct tendency for  $d_t$  to lie near one of the two values,  $2.2$  and  $5.5 \text{ \AA}$ , indicated by dashed lines in the figure. This suggests that the traps are preferentially situated in certain atomic layers of the interfacial region. The data here is

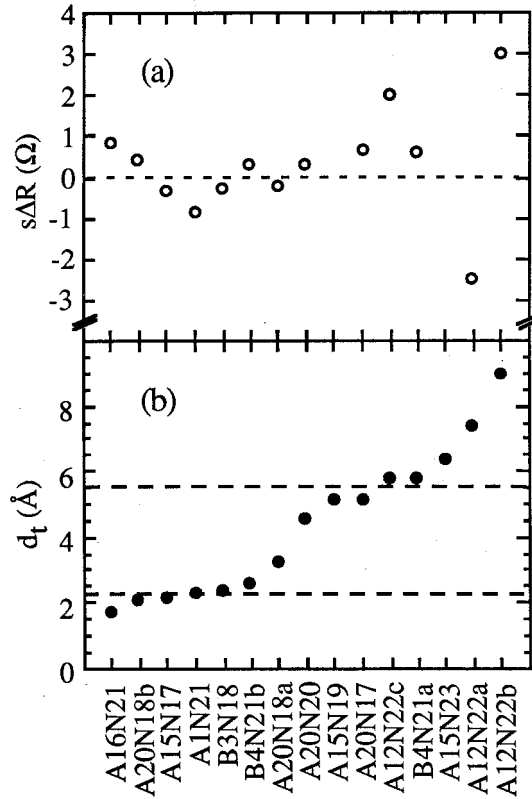


Figure 3. (a) RTS amplitude  $\Delta R$  and (b) effective depth  $d_t$  for 15 electron-trapping defects in unstressed devices at 4.2 K, sorted in order of  $d_t$ .

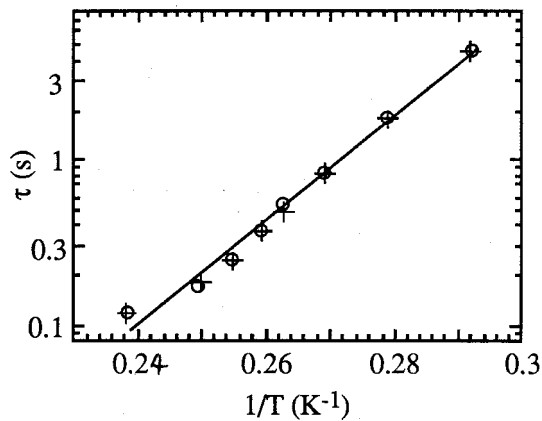


Figure 4. Temperature dependence of the time constants for an RTS in unstressed device B3N18 at  $V_g=4.74 \text{ V}$ :  $\circ \tau_1 + \tau_2$ . The straight line is the best Arrhenius fit to all points.

insufficient to establish whether the range of scattering amplitudes (ie,  $s\Delta R$ ) is different for defects at the two depths, as is possible if they have different natures and therefore different scattering amplitudes and phase shifts.

Shown in Fig. 4 are the time constants as a function of  $T$  for unstressed device B3N18 ( $d_t=2.3 \text{ \AA}$ ) at fixed  $V_g$ , chosen so that  $\tau_1=\tau_2$  at 4.2 K. Both are activated, with the same activation energy of 6 meV, so that  $\tau_1/\tau_2$  remains unity, and from Eqn. (1)  $\Delta E=E_t-E_F$  is therefore constant. As  $E_F$  is virtually independent of  $T$ , we deduce that the entropy change on electron capture is  $S_t=-\partial E_t/\partial T=0.0\pm 0.2 k_B$ . Since the only contribution to  $S_t$  which is not expected to vanish in the low temperature limit results from the change in ground-state degeneracy on electron capture, and is given by  $k_B \ln(g_1/g_2)$ , this implies that the change in degeneracy factor,  $g_1/g_2$ , is close to unity for this defect.

In stressed MOSFETs, RTSs with  $\Delta R/R$  as big as 100% are often present near threshold, and even in strong inversion  $\Delta R/R$  can be up to 10% in devices where the threshold shift is large. This is because after stress the conductance-limiting region can be so small that it is greatly influenced by the Coulomb potential from the charge of a single nearby defect. Fig. 5 shows two examples of gate-voltage sweeps in stressed devices where both RTSs and reproducible structure are present. In the main trace of Fig. 5 (a) two RTSs are visible which switch between three curves, each having a different shape. Clearly this leads to the amplitude  $\Delta R$  being a

strong function of  $V_g$ , and in one region, which is magnified in the inset,  $\Delta R$  goes through zero as the two resistance levels of one RTS cross each other. The particular form of the reproducible structure, which reflects the unique microscopic electrostatic potential landscape in the conduction-limiting region of the channel, can therefore be dramatically changed by charge trapping onto a single defect. We cannot completely rule out the possibility that the RTSs here are related to the reconfiguration of a complex of interacting defects rather than to a single trap state, but the  $V_g$  dependences are still compatible with the single-electron trapping model, although they exhibit larger values of  $d_t$ , of the order of 6 to 10  $\text{\AA}$ , than those in unstressed devices.

The time-averaged characteristic in Fig. 5 (b) shows Lorentzian peaks in the characteristics below threshold, which result from resonant tunnelling through individual localised states when the effective device length is a fraction of a micron [6]. The insets here are successive magnifications of a gate-voltage sweep over the peak at  $V_g = 3 \text{ V}$  with a high bandwidth, where a single RTS can be seen switching between curves containing similar peaks whose centres are separated in  $V_g$  by 7 mV. We infer that in this case

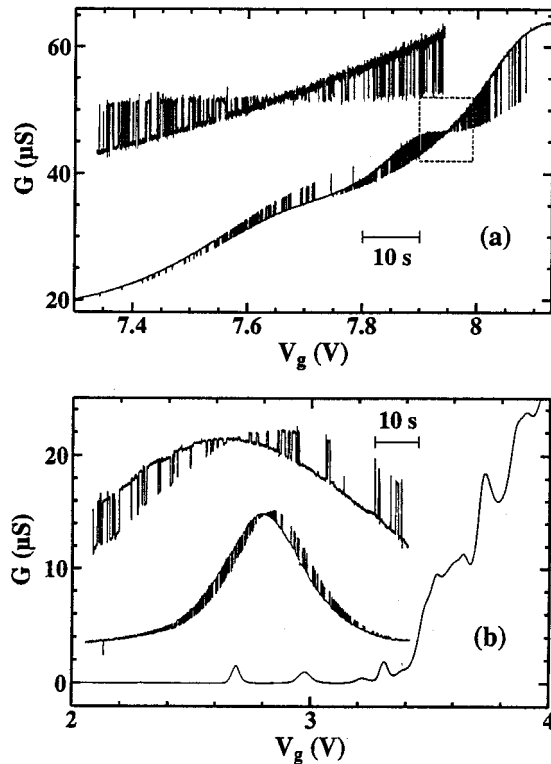


Figure 5. Gate-voltage sweeps showing RTSs in stressed devices at 4.2 K. (a) A17N24; the inset is a magnification of the boxed region on the main sweep. (b) A12N18; the insets are successive magnifications of the peak in the characteristic (main curve) at about 3 V.

the effect of an electron being trapped is principally to shift the energy of the localised tunnelling state, probably by electrostatic repulsion, with slight modifications of the tunnelling barriers into and out of the state which marginally alter the peak height.

#### 4. TWO-STATE SYSTEMS

After stressing in one particular way, with the source grounded,  $V_g$  at 3 to 5 V, and a positive drain voltage of up to 8 V applied for a second at 4.2 K, one RTS in every few devices showed a very distinctive, nonmonotonic  $V_g$ -dependence. Fig. 6 shows sweeps of  $V_g$  in a mildly stressed device in fairly strong inversion. The switching rate clearly exhibits sharp peaks at  $V_g=3.25$  V in Fig. 6 (a) and 2.81 V in (b), although  $\tau_1/\tau_2$  remains almost constant at about 1.0 in (a) and about 0.15 in (b). Fig. 7 shows  $\tau_1/\tau_2$  and the mean switching rate  $\gamma=(\tau_1\tau_2)^{-1/2}$  plotted against  $V_g$  over the whole range where the RTS was fast enough to measure.  $\tau_1/\tau_2$  follows Eqn. (1), allowing us to convert  $V_g$  to an energy scale  $\Delta E$  which is shown on the top axis. The width of the sharpest peaks is much smaller than  $k_B T$ , which is  $360 \mu\text{eV}$  at 4.2 K.

The possibility of these peaks being due to some electron capture mechanism can be excluded immediately, because the energy dependence would have to be broadened at least by the  $k_B T$  width of the Fermi distribution. However, the results are consistent with the predicted behaviour of a two-state system (TSS) coupled to an electron bath [7,8], as depicted in Fig. 8. Evidence for peaks in  $\gamma$  versus  $V_g$  was seen earlier by Schulz and Karman [9] in a p-channel device at 107 K. In that case the peak broadening was comparable to  $k_B T$ , and a model was proposed involving motion of a hole between two positions: a defect level, and a localised state in the inversion layer.

A TSS has just two quantum states, labelled 1 and 2, whose energies differ by an asymmetry energy  $\epsilon$ . The matrix element for tunnelling of the system between the two states in the absence of external influences is  $\Delta$ . The

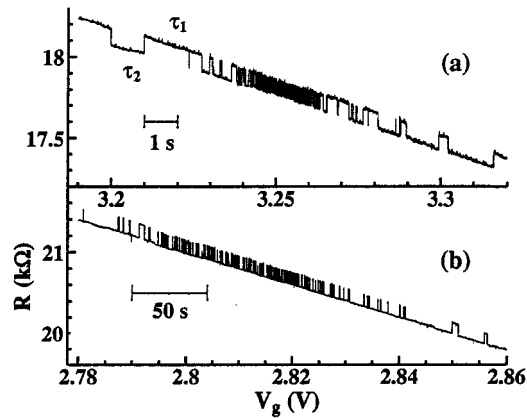


Figure 6. (a) and (b) Gate-voltage sweeps, at the indicated speeds and with a bandwidth of 1kHz, in stressed device B1N21 at 4.2 K, showing resonances in the RTS transition rate.

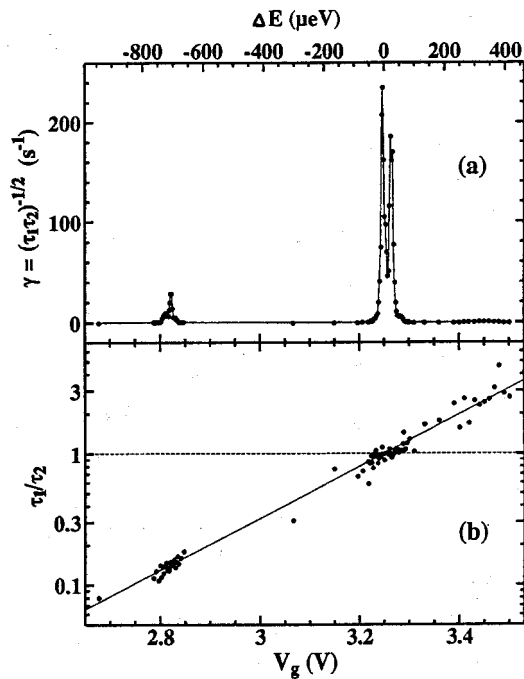


Figure 7. (a) Mean transition rate  $\gamma$  and (b) up/down ratio  $\tau_1/\tau_2$  versus gate voltage for the RTS of Fig. 6. In (a) the points are joined by straight lines. In (b) the straight line is the best fit to Eqn. (1), with  $V_{g0}=3.250$  V and  $\eta=3.6\times 10^{-3}$ , giving the energy scale marked along the top axis.

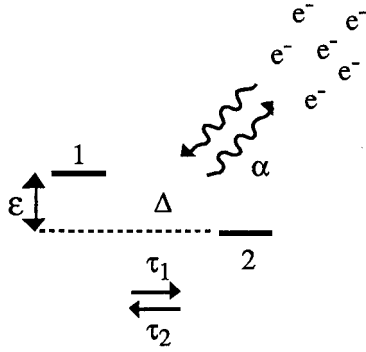


Figure 8. Schematic diagram of a two-state system coupled to an electron bath.

real system can make transitions for  $\epsilon \neq 0$  because it interacts with an external electron bath in thermal equilibrium, with a strength characterised by a coupling constant  $\alpha$ . An example of such a system is an electron tunnelling to and fro between two localised states, or an atom tunnelling between two lattice positions, in the presence of a nearby electron reservoir. Individual TSSs, with  $\alpha \approx 0.25$ , were recently shown to be the source of RTSs in thin bismuth films, and it was found that for each TSS  $\epsilon$  could be tuned in a random manner by applying a magnetic field [10]. In our systems  $\alpha$  is much smaller, of the order of  $10^{-3}$ , and we have for the first time complete control of  $\epsilon$ , which is linear in gate voltage, independently of  $\alpha$  and magnetic field. For  $\alpha \ll 1$  and  $|\epsilon| < k_B T$  it is predicted that [11]

$$\gamma(\epsilon) \approx \frac{\hbar \Delta^2}{2\pi \alpha k_B T} \frac{1}{1 + (\epsilon/2\pi \alpha k_B T)^2}, \quad (2)$$

where  $\gamma(\epsilon)$  is the geometric mean of the forward and reverse transition rates.

Figs. 9 (a) and (b) show the profile of another resonant RTS at two temperatures, 1.2 K and 4.2 K. In this case there is only one peak in  $\gamma$  which is fairly smooth and symmetric about  $V_{g0} = 1.567$  V, and whose height decreases as  $T$  increases. In Fig. 9 (b) the solid lines correspond to the best fit to Eqn. (1), with  $\eta = 3.0 \times 10^{-3}$ , and as in Fig. 7 the deduced energy scale is marked on the top axis. The curves drawn in Fig. 9 (a) correspond to the best fit to Eqn. (2), with  $\Delta E$  identified as  $\epsilon$  and  $\gamma$  as  $\gamma(\epsilon)$ , giving  $\alpha = 7 \times 10^{-3}$  and  $\hbar \Delta / k_B = 3.7 \times 10^{-5}$  K. The agreement of the fit over three orders of magnitude, and including the correct scaling of the peak height and width with temperature, is convincing evidence that the system is indeed a TSS coupled to an electron bath with  $\alpha \ll 1$ .

Fitting Eqn. (2) to the peak closest to  $\Delta E = 0$  in Fig. 7 (a) gives  $\alpha \approx 1.5 \times 10^{-3}$  and  $\hbar \Delta / k_B = 3.8 \times 10^{-6}$  K. Two other TSSs had  $\alpha \approx 2.1 \times 10^{-3}$  with  $\hbar \Delta / k_B \approx 3.4 \times 10^{-6}$  K, and  $\alpha \approx 2 \times 10^{-3}$  with  $\hbar \Delta / k_B \approx 3 \times 10^{-6}$  K. The multiple peak structure in Fig. 7 can be explained as the effect of interaction of the TSS with several other switching defects in the device, if the instantaneous value of the asymmetry energy at fixed  $V_g$  depends on the configuration of the other defects, interacting via either electric or strain fields.

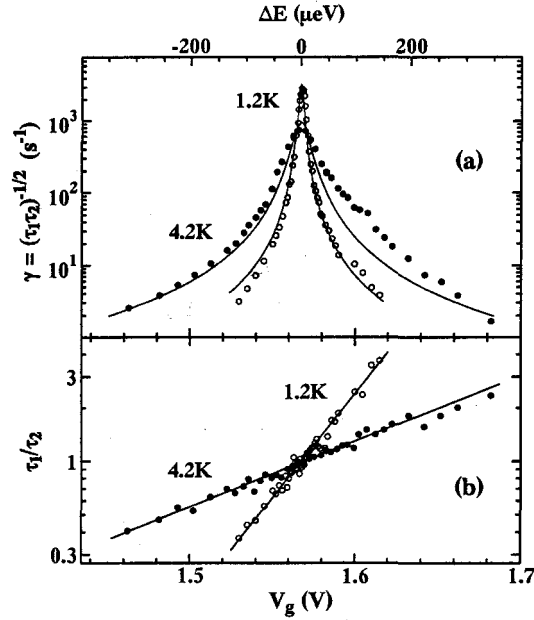


Figure 9. (a) Mean transition rate  $\gamma$  and (b) up/down ratio  $\tau_1/\tau_2$  versus gate voltage for a resonant RTS in stressed device A31N23 at 1.2 K and 4.2 K as indicated. In (a) the solid lines are the best fit to Eqn. (2), and in (b) the straight lines are the best fit to Eqn. (1).

Some splitting of the resonance peak is usual, although this is a particularly complex example, and in every case the pattern produced is different, probably reflecting the random distribution of defects.

The change in scattering cross-section, estimated from the typical value of  $\Delta R \approx 1$  to  $10 \Omega$  in strong inversion, is not inconsistent with the local interference model assuming the total cross-section is at the unitary limit [5]. Since no charge transfer is involved, we cannot infer the depth of the defect into the oxide from the value of  $\eta$ , although the large total scattering cross-section implies the defect is very close to the inversion layer electrons. Instead,  $e\eta d_{ox}$  should be the magnitude of the change in the total dipole moment parallel to the oxide electric field during the TSS transition, and eight separate TSSs had values of  $s\eta d_{ox}$  randomly distributed over the range  $\pm 1 \text{ \AA}$ . This is too small for the transition to involve motion of an electron between two separate, randomly located oxide defects. It could instead be determined by small movements of fixed charges in the lattice around the TSS, as might be expected if the TSS consisted of an atom tunnelling between two sites.

The peak switching rate at 4.2 K is never less than  $200 \text{ s}^{-1}$  and is generally of the order of  $1000$ - $5000 \text{ s}^{-1}$ , giving tunnelling matrix elements always in a rather narrow range, roughly within a decade centred on  $\hbar\Delta/k_B = 10^{-5} \text{ K}$ . Together with the limited ranges of  $\eta$  and  $\alpha$  observed, this strongly suggests that the microscopic system involved is always the same. In a mildly stressed device a TSS is hardly affected by thermal cycling from 4.2 K to room temperature, and the time-constant measurements are completely reproducible over weeks at 4.2 K. The TSS defect appears after one particular stressing process at low temperature and not after room temperature stressing. As the latter produces the dangling-bond  $P_{b0}$  and  $P_{b1}$  centres [12] in abundance, they are unlikely to be associated with the TSSs. To act as a TSS the defect needs to have two nearly degenerate ground states with a rather low overlap between them (small  $\Delta$ ). For example, some of the oxygen-vacancy related  $E'$  centres contain a hydrogen atom or a trapped hole which can sit on either of two silicon atoms, although a large lattice relaxation is expected to be necessary for the particle to move between the two states, making the transition impossible at low temperatures. However, it remains quite possible that the defect concerned has not been produced or detected in previous experiments.

## 5. CONCLUSIONS

By analysing RTSs in silicon MOSFETs at low temperatures we have found that there are intrinsic electron-trapping defects which appear to be located in specific atomic planes at the interface. Some of these defects show no change in degeneracy on electron capture, and their effect on the resistance at liquid helium temperatures is mainly not by number density modulation but by complex scattering effects. We have also discovered atomic two-state systems located near the interface, and these modulate the resistance solely by changing their scattering coefficients. These systems have much lower values of the electron coupling constant and are much more flexible than those studied before in metal films, and they present many possibilities for future investigations of the two-state system problem. They may also provide new and unusual information about the Si/SiO<sub>2</sub> interface.

## ACKNOWLEDGEMENTS

We would particularly like to thank M. Pepper and M. J. Kirton for helpful discussions, and we acknowledge the support of the UK Science and Engineering Research Council.

## REFERENCES

1. K. S. Ralls, W. J. Skocpol, L. D. Jackel, R. E. Howard, L. A. Fetter, R. W. Epworth, and D. M. Tennant, *Phys. Rev. Lett.* **52**, 228 (1984).
2. F. Koch, M. Bollu, and A. Asenov, in *Phys. and Tech. Submic. Structs.*, Eds. H. Heinrich, G. Bauer and F. Kuchar (Springer Solid-State vol. 83, Berlin, 1988).
3. M. J. Kirton and M. J. Uren, *Adv. in Phys.* **38**, 367 (1988).
4. P. A. Lee, A. D. Stone, and H. Fukuyama, *Phys. Rev. B* **35**, 1039 (1987).
5. J. Pelz and J. Clarke, *Phys. Rev. B* **36**, 4479 (1987).
6. A. B. Fowler, G. L. Timp, J. J. Wainer, and R. A. Webb, *Phys. Rev. Lett.* **57**, 138 (1986).
7. W. A. Phillips, *J. Low Temp. Phys.* **7**, 351 (1972); P. W. Anderson, B. I. Halperin, and C. M. Varma, *Philos. Mag.* **25**, 1 (1972).
8. A. J. Leggett, S. Chakravarty, A. T. Dorsey, M. P. A. Fisher, A. Garg, and W. Zwerger, *Rev. Mod. Phys.* **59**, 1 (1987).
9. M. Schulz and A. Karmann, *Appl. Phys. A* **52**, 104 (1991).
10. B. Golding, N. M. Zimmerman, and S. N. Coppersmith, *Phys. Rev. Lett.* **68**, 998 (1992).
11. This a limiting form of the general expression involving complex gamma functions given by H. Grabert and U. Weiss, *Phys. Rev. Lett.* **54**, 1605 (1985).
12. See for example A. H. Edwards, in *The Physics and Chemistry of Si and the SiO<sub>2</sub> Interface*, eds. C. R. Helms and B. E. Deal (Plenum, New York, 1988), and references therein.